Enhancement of dark and low-contrast images using dynamic stochastic resonance

Rajlaxmi Chouhan[1], Rajib Kumar Jha[2], Prabir Kumar Biswas[1]

[1]Indian Institute of Technology Kharagpur, India
[2]Indian Institute of Information Technology, Design and Manufacturing Jabalpur, India
E-mail: rajibjharajib@gmail.com

Abstract: In this study, a dynamic stochastic resonance (DSR)-based technique in spatial domain has been proposed for the enhancement of dark- and low-contrast images. Stochastic resonance (SR) is a phenomenon in which the performance of a system (low-contrast image) can be improved by addition of noise. However, in the proposed work, the internal noise of an image has been utilised to produce a noise-induced transition of a dark image from a state of low contrast to that of high contrast. DSR is applied in an iterative fashion by correlating the bistable system parameters of a double-well potential with the intensity values of a low-contrast image. Optimum output is ensured by adaptive computation of performance metrics – relative contrast enhancement factor (F), perceptual quality measures and colour enhancement factor. When compared with the existing enhancement techniques such as adaptive histogram equalisation, gamma correction, single-scale retinex, multi-scale retinex, modified high-pass filtering, edge-preserving multi-scale decomposition and automatic controls of popular imaging tools, the proposed technique gives significant performance in terms of contrast and colour enhancement as well as perceptual quality. Comparison with a spatial domain SR-based technique has also been illustrated.

1 Introduction

Contrast enhancement is required for better visualisation of dark images to improve visual perception, and to enable accurate interpretation. Many images have very low dynamic range of the intensity values because of insufficient illumination, and therefore need to be processed before being displayed. Large number of techniques have focused on the enhancement of gray-level images in the spatial domain. These methods include histogram equalisation, gamma correction, high-pass filtering, low-pass filtering, homomorphic filtering etc. [1, 2]. These methods have been also applied to colour image enhancement in the red–green–blue (R–G–B) space. Jobson *et al.* [3] have reported a retinex theory that also leads to contrast enhancement of an image. However, their technique is computationally intensive as it requires filtering with multi-scale Gaussian kernels and postprocessing stages for adjusting colours. Another technique has also been reported in R–G–B space that use equalisation of the three-dimensional (3D) histograms [4], where chromatic correlation reduction and energy compression is realised by using a multispectral Karhunen Loéve transform of the cone responses.

Noise is usually thought to be a nuisance which disturbs the system. However, recent studies have convincingly shown that in nonlinear systems, noise can induce more ordered regimes, that cause the amplification of weak signals, and increase the signal-to-noise ratio (SNR) [5–7]. Stochastic resonance (SR) is a counter-intuitive phenomenon in which noise can be used to enhance rather than hinder the system performance. In other words, noise can play a constructive role in enhancing weak signals. Noise can sometimes play a constructive role in image processing too. Recently, some of the works on application of SR for grayscale image or edge enhancement that have been reported in literature are [8–14].

The first experimental work on visualisation of SR was reported in [15]. The authors reported the outcome of a psychophysics experiment that showed that the human brain can interpret details present in an image contaminated with time-varying noise, and the perceived image quality is determined by the noise intensity and its temporal characteristics. Piana *et al.* [16] described two experiments related to the visual perception of noisy letters. The first experiment found an optimal noise level at which the letter is recognised for a minimum threshold contrast [15]. In the second experiment, they demonstrated that a dramatically increased ability of the visual system in letter recognition occurs in an extremely narrow range of noise intensity. Ye *et al.* [10] have used SR phenomenon for image enhancement of low-contrast sonar images. They have reported the image enhancement technique which showed that an additional amount of noise besides the noise of the image itself would be helpful to enhance low-contrast images. Peng *et al.* [11] reported a novel preprocessing approach to improve the low-contrast medical images using SR. The enhancement is improved by adding some suitable noise to the input image.

In this paper, an SR-based spatial domain technique for enhancement of dark- and low-contrast images has been

presented and discussed. As previous studies [7, 17] have shown that bistable SR can enhance weak 1D noisy signals, here we have extended this approach to use SR for enhancement of contrast of a 2D signal or image. An analogy of a low-contrast image to a bistable double-well dynamic system is presented and the poor state of pixel grayvalues is made to transit into enhanced state using dynamic stochastic resonance (DSR). Use of internal noise of an image has been investigated for the purpose of contrast enhancement in spatial domain.

The motivation of this study was to investigate the neutralisation of noise because of the lack of illumination using the internal noise itself. Contrast enhancement of dark images has been investigated using noise-induced SR, considering the resonance model analogous to the model developed by Benzi *et al.* [5]. Our objective is to maximise the performance of our algorithm in terms of contrast and colour enhancement while ascertaining good perceptual quality (visual information). DSR-based technique works efficiently for images that are dark as well as those which have an overall dull appearance.

The rest of the paper is organised as follows. Section 2 outlines the key contribution of the authors in the proposed work. Sections 3 and 4, respectively explain the mechanism of SR in a bistable double-well potential system, and the suitability of SR for image enhancement purposes. Sections 5 and 6 state the mathematical formulation and criteria for selection of bistable system parameters in the proposed technique respectively along with quantitative metrics used to gauge the performance. Section 7 describes the algorithm of the proposed technique, whereas results obtained from the same as displayed and discussed in Section 8. Section 9 summarises the findings of the investigation.

2 Key contribution

The work proposed in this paper is uniquely different from the state-of-the-art SR-based techniques in the aspects mentioned as follows. The technique reported in [8] deals with edge detection using vibrating noise. Also, the technique reported in [11] used non-DSR to improve the performance of adaptive histogram equalisation by using SR. The technique proposed by Ye *et al.* [10] for sonar image enhancement suggests addition of externally added noise on bi-leveled images. The authors in both [11] and [14] used the concept of non-DSR that adds N parallel frames of independent and identically distributed (i.i.d.) Gaussian noise, and uses addition of externally added noise. Our earlier work on suprathreshold stochastic resonance (SSR) [18] deals with noise-induced contrast enhancement of dark images. All these techniques are in spatial domain. However, the works reported in [12] and [13] deal with image enhancement in frequency domain, that is, Fourier and wavelet domains, respectively.

The major difference lies as follows. The focus of earlier SR-based work centred about edge detection [8], or increasing feature interpretability [10, 11, 14]. Unlike earlier techniques that were based on addition of external noise and experimental selection of parameters, the parameter selection in this work has been done by maximisation of SNR, and imposition of a condition of subthreshold nature on input image. The focus of the investigation is on real-life dark images, and it is here that a noise-enhanced DSR-based application in pixel intensity domain has been investigated for the first time. In the

proposed technique, noise itself is used to counter the effect of noise. In other words, a small amount of extra noise rearranges the intrinsic noise that is already present in the image. Contributing and novel aspects of this work are: adaptively ensuring maximal performance of the DSR-based algorithm in terms of contrast and colour enhancement alongside assuring good perceptual quality (visual information), and the analysis of mechanism of DSR on intensity distribution of dark images.

An enhancement model analogous to the double-well model proposed by Benzi *et al.* [5, 19] has been presented. The proposed model treats each pixel as a discrete particle, and its intensity value as a kinetic parameter of the motion of the particle in a double-well system. Since the subthreshold property of input signal is essential in a DSR-exhibiting system, a dark- and low-contrast images, with very less variance in amplitude of intensity values fits well as a subthreshold signal. A transition of the image from the low-contrast state to high-contrast state is induced by a 'noise-induced' resonance between the internal noise and subthreshold signal after certain number of iterations, following the dynamics of motion of a particle in a double-well. Oscillations about the mean (minima) of the double-well are considered analogous to iterations of the discrete resonance equation. The proposed technique follows an adaptive algorithm and selects best output when performance metrics are maximal. The proposed technique selects parameters by maximisation of SNR and also further relates the DSR parameters with the statistical properties of the low illuminated image itself. The applicability of DSR has been extended on a low-contrast image (to make it a subthreshold signal) by imposing condition on another double-well parameter so that the coefficients of low-contrast image can be accepted as an input signal for this image enhancement technique.

In an RGB image, each pixel is specified by three values – one each for the red, blue, and green components of the pixel's colour. MATLAB stores RGB images as an $m{\times}n{\times}3$ data array that defines red, green and blue colour components for each individual. Another way of making the same colours is to use their hue (pure colour), their saturation (colourfulness of a stimulus relative to its own brightness) and their brightness value (subjective brightness perception of a colour). This is called the hue–saturation–value (HSV) colour space. To ensure implicit colour preservation, HSV has been used instead of RGB colour space, and DSR is applied to value vector, V, in the projected colour space.

3 Dynamic stochastic resonance

The concept of SR was invented in 1981–1982 in the context of the evolution of the Earth's climate. Statistical data show that interglacial transitions can be considered to be a random variable displaying average periodicity of around 10^6 years. Since the only known time scale in this range is that of the changes of the eccentricity of the Earth's orbit around the Sun, as a result of the perturbing action of the other bodies of the solar system. This perturbation modifies the total amount of solar energy received by the Earth, but the magnitude of this astronomical effect is exceedingly small, about 0.1%. The search for a answer to explain how such a small change in eccentricity can cause such drastic changes in temperature led to the concept of SR. In the model of Benzi *et al.* [5, 19] to explain recurrence of ice

age on Earth, the global climate was represented by a double-well potential, where one minimum represents a small temperature corresponding to a largely ice-covered Earth. The small modulation of the Earth's orbital eccentricity is represented by a weak periodic force. Short-term climate fluctuations, such as the fluctuations in solar radiation, are modelled by Gaussian white noise. If the noise is tuned accordingly, synchronised hopping between the cold and warm climates could significantly enhance the response of the Earth's climate to the weak perturbations caused by the Earth's orbital eccentricity. Starting in the late 1980s the ideas underlying SR were taken up, elaborated and applied in a wide range of problems in physical and life sciences [5, 15, 20].

SR is a phenomenon where the input signals of some nonlinear systems can be amplified by the addition of optimum amount of noise. More technically, SR occurs if the SNR, input/output correlation have a well-marked maximum at a certain noise level. This concept was extensively studied and comprehensively reviewed by the authors [7, 17].

In order to exhibit SR, a system should possess three basic properties: a nonlinearity in terms of threshold, a sub-threshold signal like a signal with small amplitude and a source of additive noise. This phenomenon occurs frequently in bistable systems, or in systems with threshold-like behaviour. The general behaviour of SR mechanism shows that at lower noise intensities the weak signal is unable to cross the threshold, thus giving a very low SNR. For large noise intensities the output is dominated by the noise, also leading to a low SNR. However, for moderate noise intensities, the noise allows the signal to cross the threshold giving maximum SNR at some optimum noise level. Thus, a plot of SNR as a function of noise intensity shows a peak at an optimum noise level as shown in Fig. 1a.

The bistable-SR model conventionally used by the physicists shall be explored and elaborated for application to contrast enhancement of a digital image. In analogy to Benzi's double-well model to explain ice ages, the image pixel value is treated like a discrete kinetic parameter, say, the position of a particle in the double well. For a low-contrast image, the analogy states that the pixel is initially in a weak signal state (because of low-intensity value since image is low contrast, i.e. a subthreshold signal). Addition of optimum amount of noise effects its transition to the strong signal state (high contrast), just as a particle makes a transition from one well to another. Such a change of state of pixel under noise can be modelled by Brownian motion of a particle placed in a double-well potential system shown in Fig. 1b.
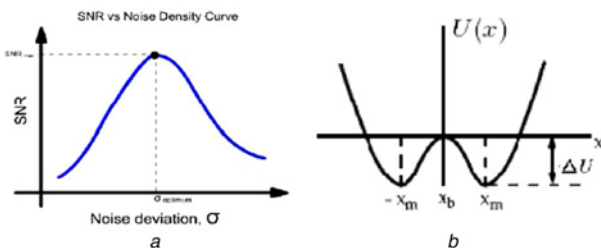
A classic 1D nonlinear dynamic system that exhibits SR is modelled with the help of the Langevin equation of motion given in [21] in the form of (1) given below

$$m\frac{d^2x(t)}{dt^2} + \gamma\frac{dx(t)}{dt} = -\frac{dU(x)}{dx} + \sqrt{D}\xi(t) \qquad (1)$$

This equation describes the motion of a particle of mass m moving in the presence of friction, γ. The restoring force is expressed as the gradient of some bistable potential function $U(x)$. In addition, there is an additive stochastic force $\xi(t)$ of intensity D.

If the system is heavily damped, the inertial $md^2x(t)/dt^2$ term can be neglected. Rescaling the system in (1) with the damping term γ gives the stochastic overdamped Duffing equation [22], which is frequently used to model non-equilibrium critical phenomena as given in (2)

$$\frac{dx(t)}{dt} = -\frac{dU(x)}{dx} + \sqrt{D}\xi(t) \qquad (2)$$

where $U(x)$ is a bistable quartic potential (Fig. 1a) given in (3)

$$U(x) = -a\frac{x^2}{2} + b\frac{x^4}{4} \qquad (3)$$

Here, a and b are positive bistable double-well parameters. The double-well system is stable at $x_m = \pm\sqrt{(a/b)}$ separated by a barrier of height $\Delta U = (a^2/4b)$ when $\xi(t)$ is zero.

The Langevin equation describes the motion of particle in a general double-well. However, in our case of image domain, for mathematical simplicity, the damped system neglecting inertial terms of the Langevin equation has been considered (2).

The relation of parameters in this equation with an image model is as follows: since $(dx(t))/(dt)$ represents rate of change of particle position in the double-well, in image domain it may represent information indicating frequency of graylevel changes of the same pixel. Since $U(x)$ represents the quartic potential function of x, and defines the shape of the double-well with values of parameters a and b as given in (3), $U(x)$ may, therefore be considered to represent image contrast, where position $-x_m$ and $+x_m$ represent two states of the contrast (where $\pm x_m$ are the minima of the double-well). $\sqrt{D}\xi(t)$ may represent the internal or externally added noise function, denoted by $\xi(t)$ and having a noise deviation, $\sqrt{D}$. With these model analogies, the double-well model maybe used to replicate instances of double-well scenario in image domain.

Continuing with the mathematical formulation of SR, the dynamics of the SR system are described as follows. Addition of a periodic input signal $[B \sin(\omega t)]$ to the bistable system makes it time-dependent whose dynamics are governed by (4)

$$\frac{dx(t)}{dt} = -\frac{dU(x)}{dx} + B\sin(\omega t) + \sqrt{D}\xi(t) \qquad (4)$$

where B and ω are the amplitude and frequency of the periodic signal, respectively. It is assumed that the signal amplitude is small enough so that in the absence of noise it

Fig. 1 *SR in double-well potential valley*

a SNR against noise density
b Bistable double-well potential system

is insufficient to force a particle to move from one well to another.

The bistable potential, which is now time-dependent, becomes

$$U(x, t) = U(x) - Bx \sin(\omega t)$$
$$= -a\frac{x^2}{2} + b\frac{x^4}{4} - Bx \sin(\omega t) \quad (5)$$

Substituting $U(x)$ from (3) into (4)

$$\frac{dx(t)}{dt} = [ax - bx^3] + B\sin(\omega t) + \sqrt{D}\xi(t) \quad (6)$$

In the absence of periodic force, the particle fluctuates around its local stable states. The rate of transition of particle (r_k) between the potential well under the noise-driven switching is given by Kramer's rate [21] as in (7)

$$r_k = \frac{a}{\sqrt{2}\pi} \exp\left[-\frac{2\Delta U}{D}\right] \quad (7)$$

When a weak periodic force is applied to the unit mass particle in the potential well, noise-driven switching between the potential wells takes place and is synchronised with the average waiting time, $T_k(D) = (1/r_k)$, between two noise-driven inter-well transitions that satisfies the time-scale matching between signal frequency ω and the residence times of the particle in each well [7, 23]. That is

$$2T_k(D) = T_\omega \quad (8)$$

where T_ω is the period of the periodic force.

The most common quantifier of SR is SNR. The SNR expression for DSR as derived in [9] is given below

$$SNR = \left[\frac{4a}{\sqrt{2}(\sigma_0 \sigma_1)^2}\right] \exp\left(-\frac{a}{2\sigma_0^2}\right) \quad (9)$$

Here σ_1 is the standard deviation of the added noise in the SR-based system, and σ_0 is the internal noise standard deviation of the original bistable system.

4 Choice of DSR for image enhancement

To utilise the principles of physics in image processing, the discrete image pixels are incisively treated as discrete particles, whereby the grayvalue of an image pixel corresponds to a specific kinetic parameter of a physical particle in Brownian motion. An analogy to Benzi et al.'s double-well model (for global climate) in the context of image enhancement has been developed in this paper. Here double well represents the contrast of an image. The position of particle is analogous to the state of the intensity values. The weak periodic force is constituted by the grayvalues, whereas noise is constituted by the noise inherent in the graylevel distribution because of lack of illumination. Each of the two stable states are represented by a low-contrast state and enhanced state respectively. The state at which performance metrics are found to be optimal

can be considered the state after one hopping to enhanced state from input state. On increasing the number of iteration beyond optimum, it can be said to be in a state when the motion (inter-well transition) between two stable states becomes oscillatory.

DSR is exhibited by a double-well potential system denoted by parameters a and b that signify the state of such a system. The double-well with two stable states can be used to suggest two states of an image – one in which its overall energy is low, and one in which it is high. The transition from one state to another can be modelled by addition of weak noise (in our case, the internal noise). The image pixels of a low-contrast image are said to be in poor state in the sense that their graylevel distribution is affected by inherent noise in the form of lack of proper illumination. When each grayvalue is tuned using DSR, the spread of graylevel distribution increases causing the overall contrast of an image to increase. The result is that an image in low-contrast state transits into a high-contrast state after certain optimum number of intra-well oscillations (iterations).

SR has been established earlier in applications of image enhancement by the authors [11–13, 18]. The fact that SR can enhance a weak subthreshold signal, and an image with low-contrast can be modelled as one, we chose DSR for contrast enhancement. Our earlier work that includes application of non-DSR on enhancement of dark images [18] is based on the principle of SSR. It uses addition of external noise in spatial domain, where many frames of i.i.d random noise (of some noise deviation) are added to an image, and the noisy images are successively hard-thresholded followed by overall averaging. By varying the noise deviation, external noise-induced resonance is obtained at a particular optimum noise intensity. However, this approach is a special case (and a relatively crude form) of SR in the view of the nonlinearity involved. The type of nonlinearity introduced in the SSR-based approach is because of thresholding, whereas in DSR, it is because of barrier height of double-well. In SSR, the resonance breaks up the harmonic distortion (quantisation) because of the threshold operation by spreading the distortion across the spectrum, and the integration (averaging) eliminates much of the noise that has been pushed into higher spatial frequencies. However, to achieve this with high efficiency, a large number of averaging frames are required. This gives us the motivation to pursue the dynamic form of SR, where larger efficiency in performance may be achieved by using double-well parameters. Scaling of intensity values following an iterative equation allows tuning of parameters to suit our requirement, and also helps in observing the incremental enhancement obtained in every iteration. The extent of computation required is also less because large number of frames need not be processed for each value of noise deviation.

It may be well noted here, that the difference between internal noise and external noise is primarily because of the mode following which noise is added to a noise-free image. An image with appropriate illumination and good perceptual quality may be considered to have little or no noise. However, an image taken under poor illumination does not adequately represent the object perceptibility in the scene. Such an image may be considered to be noisy in the sense that the property of low-contrast may be modelled as degradation that decreases the perceptibility of objects in the scene. This is how lack of illumination may be considered as internal noise of a low-contrast/dark image. To process such an image using DSR, if noise is added

externally during the iterative step to induce resonance, it is termed as external noise-induced resonance, whereas if the internal noise is iteratively scaled, it is termed to be internal noise-induced resonance.

5 Mathematical formulation of the DSR-based contrast enhancement

Mathematical formulation of DSR for enhancement of very dark image is discussed here. The explanation as to how the dynamic equation can be formulated to model a static image has already been explained in Section 3 at the introduction of dynamic equations. Let us consider the 2D spatial representation of an image $I(x, y)$ in an actual physical space (x, y) where the function I will be image pixel value.

DSR is applied to $I(x, y)$ (grayscale image), or value vector, $V(x, y)$, (in H–S–V space), thereby obtaining the stochastically enhanced set of graylevel values (enhanced image) given as

$$V(x, y)_{\text{enhanced}} = \text{DSR}[V(x, y)] \qquad (10)$$

where the DSR operation can be shown in differential equation form and in discrete equation form as given in (6) and (11).

Here, the noise term $\sqrt{D}\xi(t)$ and the input term $B \sin(\omega t)$ is replaced by intensity values of $I(x, y)$. In (6), DSR is induced by the noise term $\sqrt{D}\xi(t)$, whereby the maximisation of the SNR occurs at double-well parameters $a = 2\sigma_0^2$ (as described in Section 6).

We now computationally implement the DSR in digital images. We need to solve the stochastic differential equation given in (6) using the Euler–Maruyama's method of the iterative discretisation as follows [24]

$$x(n + 1) = x(n) + \Delta t \big[ax(n) - bx^3(n) + \text{input}\big] \qquad (11)$$

Note that, input $= B \sin(\omega t) + \sqrt{D}\xi(t)$ denotes the sequence of input signal and noise. This denotation can be done with the view that the low-contrast image is a noisy image containing internal noise because of lack of illumination. This noise is inherent in its intensity distribution, and therefore the intensity value vector, V, can be viewed as containing signal (image information) as well as noise. The final stochastic simulation is obtained after certain number of iterations.

6 Selection of parameters for image enhancement

This section describes one of our key contributions – the approach for selection of double-well system parameters a and b.

6.1 Selection of a

SR is observed by (11) after proper selection of the double-well parameters a and b. These double-well parameters can be obtained by maximisation of the SNR expression.

For SNR maximisation, we differentiate (9) with respect to a and equal to zero. Out of two parameters a and b of the

DSR, any one can be selected for discussion. We have selected parameter a here for our discussion

$$\frac{\text{d(SNR)}}{\text{d}(a)} = \left[\frac{1}{\sqrt{2}(\sigma_0\sigma_1)^2}\right] \exp\left(-\frac{a}{2\sigma_0^2}\right)$$
$$- \left[\frac{a}{\sqrt{2}(\sigma_0\sigma_1)^2}\right]\left(\frac{1}{2\sigma_0^2}\right) \exp\left(-\frac{a}{2\sigma_0^2}\right) = 0 \qquad (12)$$

This gives $a = 2\sigma_0^2$ for maximum SNR. Thus SNR has maximum value at an intrinsic property a of the double-well system.

6.2 Selection of b

To ensure that the low-contrast image is a subthreshold signal, a condition for the value of parameter b has been derived. As shown in (1), the restoring force is expressed as the gradient of some bistable potential function $U(x)$. We have arrived at the maximum possible value of such an additive periodic signal so that the bistable potential well remains stable. Let $R = B \sin \omega t$ be the periodic signal

$$R = -\frac{\text{d}U(x)}{\text{d}x} = -ax + bx^3, \frac{\text{d}R}{\text{d}x} = -a + 3bx^2 = 0 \qquad (13)$$

implying $x = \sqrt{(a/3b)}$. Finding R at this value gives maximum force as $\sqrt{(4a^3/27b)}$. This is the maximum possible force at which the bistable system would remain stable. At a force larger than this, the system would become unstable. Therefore

$$B \sin \omega t < \sqrt{\frac{4a^3}{27b}} \qquad (14)$$

Since our desire is to obtain a maximal signal, we let the sine term attain its maximum value, that is, unity. Since $B \sin \omega t$ is to be a subthreshold signal, its maximum amplitude, B, can also be assumed to be unity for mathematical simplicity

$$1 < \sqrt{\frac{4a^3}{27b}} \qquad (15)$$

Therefore, for weak input signal $b < (4a^3/27)$.

Therefore the values of these parameters for maximising contrast enhancement or SNR (in a general sense) are taken to be $a = 2\sigma_0^2$ and $b < (4a^3)/27$.

6.3 Quantitative performance metrics

Performance measures such as peak signal-to-noise-ratio (PSNR), mean-square-error (MSE), structural similarity index measure, quality index etc. are not suitable for our purpose. These measures require distortion-free image or reference image. Such images are not available in the current context. Since we need to gauge the performance of our technique in terms of contrast as well as perceptual quality, we have chosen two metrics, relative contrast enhancement factor (F) and perceptual quality metric (PQM), respectively, to characterise each of them. However, for the standard test images that were originally of normal contrast and were manipulated to be made dark

for investigation of the technique, we have tabulated the MSE and PSNR values.

Metric of contrast enhancement (F) is based on global variance and mean of original and enhanced images. It can be stated that when an image is enhanced and clearer heterogeneity in its structure is obtained, the value of enhancement can be characterised by variation of Michelson contrast index (which is given by ratio of spread and mean image intensity) [13]. We have therefore used a descriptor called image contrast quality index, Q, such that

$$Q = \frac{\sigma^2}{\mu} \qquad (16)$$

where σ and μ are, respectively, the standard deviation and mean of the image. An estimate of relative contrast enhancement factor, F, can be obtained by computing ratio of values of quality index post-enhancement (Q_B) and pre-enhancement (Q_A). Therefore

$$F = \frac{Q_B}{Q_A} \qquad (17)$$

For evaluation of perceptual quality, we have used a no-reference metric for judging the image quality taking into account visible blocking and blurring artifacts, which we shall refer to as PQM [25]

$$PQM = \alpha + \beta B^{\gamma_1} A^{\gamma_2} Z^{\gamma_3} \qquad (18)$$

where α, β, γ_1, γ_2 and γ_3 are model parameters that were estimated with the subjective test data as described by [25] ($\alpha = -245.9$, $\beta = 261.9$, $\gamma_1 = -0.0240$, $\gamma_2 = 0.0160$ and $\gamma_3 = 0.0064$). B is the average blockiness, estimated as the average differences across block boundaries for horizontally and vertically. A and Z constitute the activity of the signal. Although blurring is difficult to be evaluated without the reference image, it causes the reduction of signal activity. A is the average absolute difference between in-block image samples and Z is the zero-crossing rate. The code available at [26] has been used to compute the metric PQM. According to Mukherjee and Mitra [27], the PQM value should be close to 10 for best perceptual quality.

Since, we are also interested to observe the quality in terms of colour enhancement, we have used a no-reference metric called colourfulness metric (CM) as suggested by Susstrunk and Winkler [28]. If R, G and B be the red, green and blue components respectively of an image I and let $\alpha = R - G$ and $\beta(R + (G/2)) - B$, then the colourfulness of the image is defined as follows

$$CM(I) = \sqrt{\sigma_\alpha^2 + \sigma_\beta^2} + 0.3\sqrt{\mu_\alpha^2 + \mu_\beta^2} \qquad (19)$$

where σ_α and σ_β are the standard deviations of α and β. Similarly, μ_α and μ_β are their means. Color enhancement factor (CEF) is defined as the ratio of colorfulness of enhanced image to that of original image.

7 Proposed algorithm

The schematic diagram showing the steps in the DSR-based algorithm for contrast enhancement has been shown in

Fig. 3a. The following algorithm has been described for an RGB image. In case the input is a grayscale image, the same operation is performed on the intensity matrix (omitting the steps of colour conversion).

Step 1. Conversion of RGB image to HSV colour space: This conversion is performed to minimise the computation complexity, and to ensure implicit colour preservation of the image.

Step 2. Application of DSR: The intensity values (graylevels) are tuned using DSR as follows. Find the standard deviation of the intensity values of the dark- or low-contrast input image, σ_0. Assume $\Delta t = 0.01$, $a = 2\sigma_0^2$, $b = 0.00001 \times (4a^3)/27$. A fractional factor (much less than 1) has been multiplied to ensure that b is less than its maximum value to ensure that input is subthreshold signal and eligible for application of DSR (as discussed in Section 6.2).

Initialising a matrix of dimension $M \times N$ as zero. $x(0) = 0$.

Using the bistable DSR parameters tune the graylevel values according to (11) as

$$x(n + 1) = x(n) + \Delta t[ax(n) - bx^3(n) + V] \qquad (20)$$

where $x(n + 1)$ denotes set of tuned coefficients after $n + 1$ iterations. Here V is the low-contrast image intensity (value) vector or the graylevel matrix itself (in case of a grayscale image).

Step 3. Adaptive Iteration: Compute the new RGB image (after each iteration) using the initial hue and saturation vectors and the DSR-tuned value vector, x. To make the algorithm adaptive, the performance metrics $F(n)$, $PQM(n)$ and $CEF(n)$ of x are calculated after each iteration. Assuming initial values of each of these parameters as 0.0001. Since the metrics are computed after each iteration, the iterative process is continued till $F(n) + CEF(n)$ becomes maximum within the constraint that PQM is as close as possible to value 10.

8 Experimental results and discussion

The proposed DSR-based technique was tested on a dataset of around 40 random dark- and low-contrast images. Twenty of those imagess were naturally dark, (e.g. Figs. 2a, c, and 3b), whereas ten were made poor contrast by manipulation (e.g. Figs. 3d and 5a–d). Ten of the remaining test images were originally low-contrast; for example, the input image as shown in Fig. 6a is of dull appearance and low-contrast and has been taken directly from [29]. Experimental results obtained using the proposed algorithm have been shown in Figs. 2–5. Optimisation characteristics with respect to iteration is shown in Figs. 6c–d. Figs. 5a–d shows original standard images; Figs. 5e–h shows dark- and low-contrast images obtained by manipulation of Figs. 5a–d for the purpose of testing the enhancement technique. Figs. 5i–l shows DSR-based results on the respective dark images. For test image Lena (Fig. 5e), $n = 11$ is found to be the optimum number of iterations. The nature in which the iterative equation modifies the distribution of intensity values of a low-contrast image is shown in Figs. 4. The platform used for software simulation is MATLAB v.7.0.4, on Windows XP with on Intel(R)Core(TM) 2 Duo CPU E7200 @ 2.53 GHz with 1.98 GB of RAM.

The striking feature of the proposed DSR-based technique is its treatment of even very dark images. It should be noted here that the effect of DSR inherently scales each of the intensity values with a factor nonlinearly proportional to its
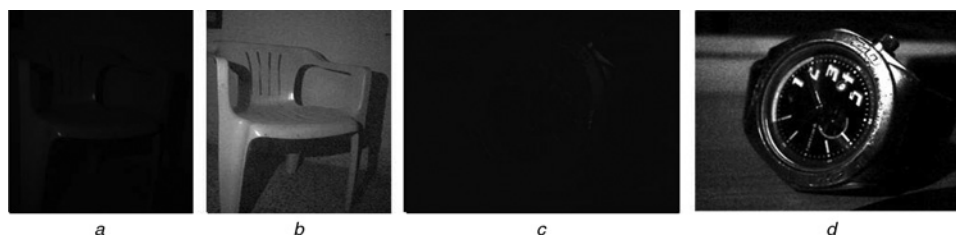
Fig. 2 *Two naturally dark input images taken in poor illumination*

DSR-enhanced output shows remarkable improvement in image information
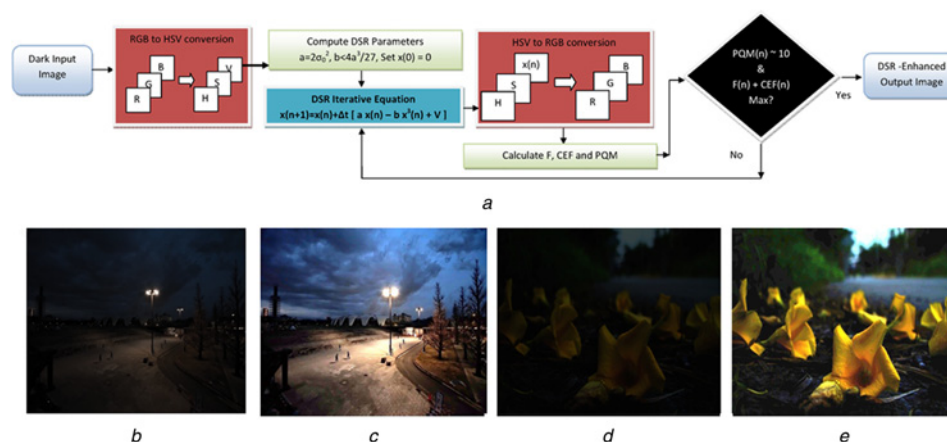

Fig. 3 *Schematic of the DSR-based enhancement algorithm on pixel values*

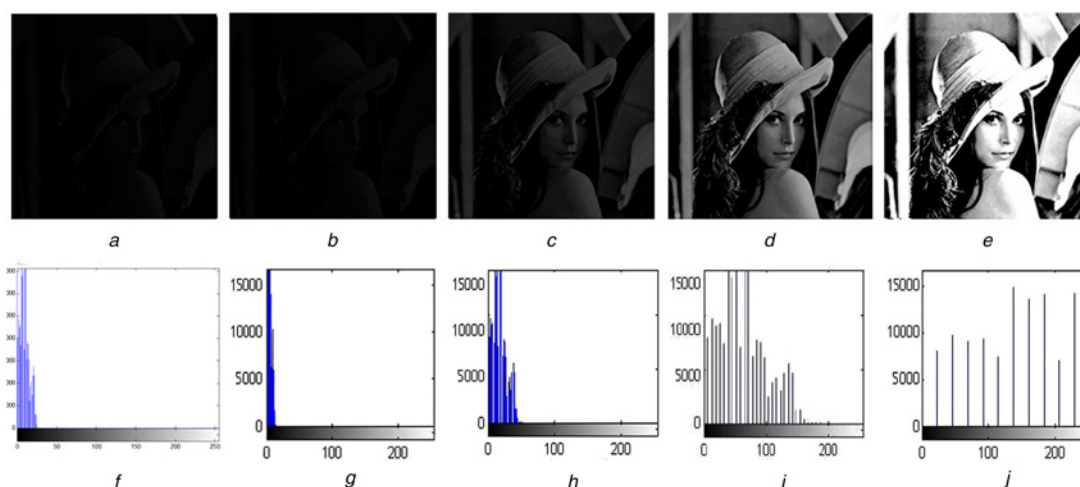DSR-enhanced output shows remarkable improvement in image information and colourfulness

Fig. 4 *Mechanism of the DSR iterative equation on intensity distribution of a dark image*

a and *e* Respectively show a dark input image and its intensity distribution
b–e and *g–j* Respectively show the output image and their intensity distributions after applying 6, 8, 10 and 12 DSR iterations

internal noise. By directly operating in spatial domain or pixel intensity values, DSR causes the distribution of intensity values to be broadened, and increases the dynamic range of the image by correlating the parameters of a bistable double-well potential system with the intensity values. The transition of the image from a poor contrast state to a good contrast state is reflected by one hopping from one minima of the double-well to another after certain number of oscillations about the mean position of minima, here reflected in terms of number of iterations. Various other characteristics of the proposed DSR technique for contrast enhancement have been discussed in this section.

8.1 Effect of DSR on intensity distribution

It can be seen in Fig. 4 that the intensity distribution (histogram) of a dark image is narrow and concentrate at the lower (darker) end of the intensity scale. It can be observed that with each iteration, intensity values are scaled with a factor proportional to the noise inherent in the image itself. As a result, the spread (standard deviation) of the distribution increases, and the mean shifts towards the higher end. This change is reflected in the output image as increase in brightness (mean) and improvement of contrast (standard deviation). This is how DSR works on both

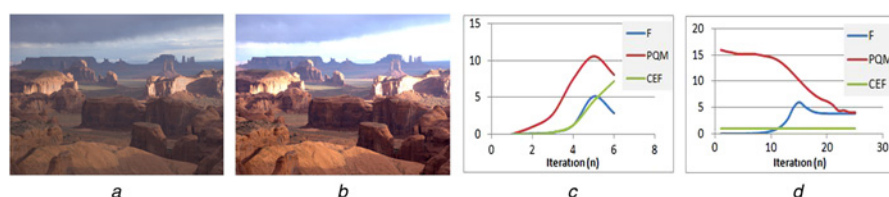**Fig. 5** *DSR-enhanced output on some standard test images (made dark- and low-contrast by manipulation)*

Fig. 6 *DSR-enhanced outputs and performance characterisation*
a and *b* DSR-enhanced output shows remarkable improvement in image information and colourfulness
c and *d* Variation of performance metrics w.r.t. iteration count, *n*, for a dark images

dark- and low-contrast images to enhance the contrast as well as perceptual quality.

8.2 Comparative analysis

Outputs of comparison with other existing image enhancement techniques has been shown in Figs. 7 and 8.

In spatial domain, comparison with contrast-limited adaptive histogram equalisation (CLAHE) [30], gamma correction (Gamma) [1], single-scale retinex (Retinex) [3], multi-scale retinex (MSR) [31] modified high-pass filtering (MHPF) [32] and edge-preserving multiscale decomposition (EPMD) [29] has been done. A comparison with another SR-based technique (non-dynamic) [18]
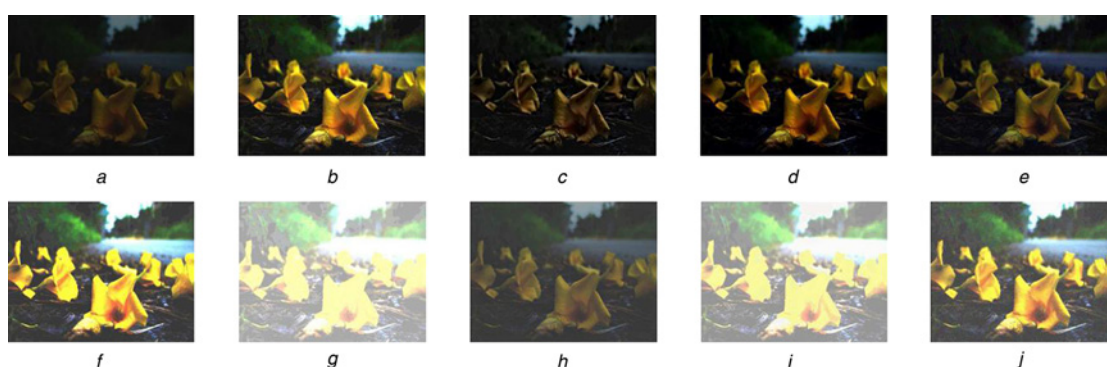

Fig. 7 *Enhancement results on a low-contrast input image using proposed DSR-based technique and other existing enhancement techniques*
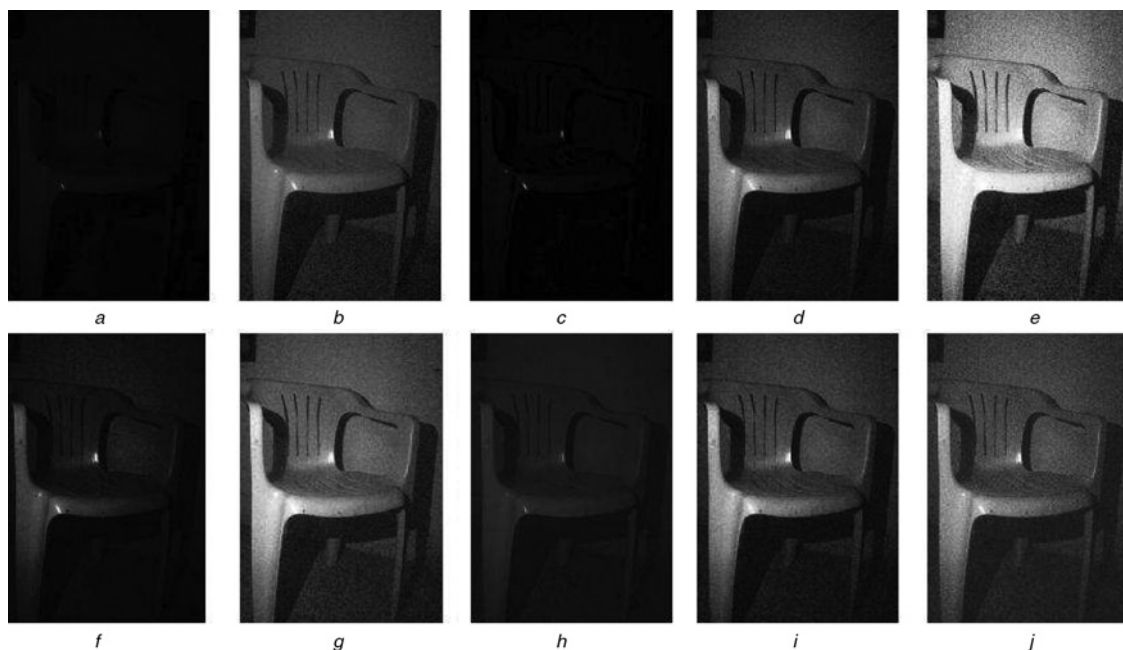
Fig. 8 *Enhancement results on a very dark input image using proposed DSR-based technique and other existing enhancement techniques*

has also been shown. Since the proposed technique is an automatic algorithm comparison has been made with outputs of 'Auto Contrast' control of Adobe Photoshop CS2. The medium detail of EPMD [29] was used as obtained from [33].

8.3 Performance evaluation

The performance values have been tabulated in Tables 1 and 2. Values for the proposed DSR-based algorithm have been displayed in bold in Tables 1 and 2 to highlight its

Table 1 Comparative performance of the proposed technique with various existing techniques using two performance metrics F [13] and PQM [25] on three grayscale input images

Methods	Fig. 2a		Fig. 4a		Fig. 2c	
	F	PQM	F	PQM	F	PQM
DSR	**7.643**	**9.903**	**8.731**	**9.707**	**12.936**	**10.128**
CLAHE [30]	21.384	8.718	3.954	9.161	6.812	8.056
Gamma [1]	7.278	12.509	5.304	8.794	6.514	11.231
Retinex [3]	14.589	10.969	9.864	8.966	1.481	11.133
MSR [32]	1.648	13.292	2.848	8.795	0.598	6.407
MHPF [32]	14.076	11.319	0.982	6.701	2.689	11.734
EPMD [29]	2.037	9.881	0.824	9.642	0.8541	9.642
Photoshop	13.615	10.733	10.601	9.315	9.401	12.509

Figs. 2a and c are naturally dark images, whereas Fig. 4a has been made dark- and low-contrast by manipulation

Table 2 Comparative performance of the proposed technique with various existing techniques using three performance metrics F [13], CEF [27] and PQM [25] on three coloured input images

Methods	Fig. 3b			Fig. 3d			Fig. 6a		
	F	PQM	CEF	F	PQM	CEF	F	PQM	CEF
DSR	**3.54**	**9.76**	**3.09**	**5.18**	**10.57**	**4.52**	**1.769**	**10.31**	**1.65**
CLAHE [30]	2.18	10.39	1.26	2.38	8.72	2.57	3.21	10.57	1.26
Gamma [1]	1.22	10.95	1.48	4.1	8.69	4.59	1.16	10.92	1.48
Retinex [3]	0.09	12.37	0.27	0.50	8.76	2.16	0.087	12.24	0.27
MSR [31]	0.37	11.67	0.72	0.59	8.29	1.27	0.36	11.77	0.72
MHPF [32]	0.60	11.55	0.84	0.77	10.70	2.56	0.62	11.64	0.83
EPMD [29]	2.45	10.19	0.93	2.28	8.58	1.12	2.75	10.19	0.93
Photoshop	2.05	11.01	1.25	6.15	11.28	2.73	2.01	11.03	1.25
SSR [18]	6.10	8.95	5.11	2.35	9.74	6.6	2.01	10.65	1.98

Fig. 3b is a dark image. Figs. 3d and 6a are low-contrast images

Table 3 MSE and PSNR between original unmanipulated standard images, manipulated dark images and DSR-enhanced images

Image	Original and DSR		Original and dark		DSR and dark	
	MSE ($\times 10^3$)	PSNR, dB	MSE ($\times 10^3$)	PSNR, dB	MSE ($\times 10^3$)	PSNR, dB
Fig. 5a	4.08	11.67	15.5	5.88	18.93	6.22
Fig. 5b	1.18	17.4	16.0	6.09	23.8	4.35
Fig. 5c	5.37	9.85	11.1	6.72	7.9	9.5
Fig. 5d	4.09	11.12	15.9	5.08	11.02	7.71

Table 4 Comparative values of double-well parameter a, with corresponding required number of iterations, n to reach high target performance value

Parameter a	Iteration count required (n)
20	295
40	212
60	150
80	94
85	59
88$(= 2\sigma_0^2)$	**11**
100	33
120	79

performance, and to distinguish its performance from other techniques compared with. Original noise-free images were available for some images that were manipulated and made dark for investigation of the proposed technique. Since such images are being made dark on purpose, this can be considered to be addition of noise to an originally noise-free image, as in the case of a phantom image. To indicate the relative removal of such 'degradation' in the DSR-enhanced image, we have calculated the MSE and PSNR between (a) original un-manipulated image and DSR-enhanced image (original–DSR), (b) original un-manipulated image and manipulated (dark) image (original–dark) and (c) DSR-enhanced image and manipulated (dark) image (DSR–dark) (Table 3). It was observed that the MSE between DSR-enhanced image and original image is far less than that between original and dark images, as well as enhanced and dark images. This validates the fact that the noise added because of manipulation in the image, has been removed to a great extent in the enhanced image.

- *Contrast enhancement factor (F):* It is clear from the values that the proposed DSR-based technique gives reasonably high-contrast enhancement factor (F) values for almost all the images; the same is apparent from the visual output images.
- *Colour enhancement factor (CEF):* For coloured images, it can be observed the the colourfulness of output image is greater than that of input for both dark- and low-contrast images.
- *Perceptual quality measure (PQM):* As stated in Section 6.3, *PQM* should be close to 10 for best perceptual quality. It should be noted here that diversion away from 10 on either direction is an indication on decrease in perceptual quality. For this, value of *PQM* for the proposed technique is second only to [29] technique on a well-illuminated but low-contrast image. On darker images, the DSR-based technique keeps the *PQM* closest to 10, signifying better perceptual quality than most of the other techniques.

It is a common observation that most of the existing techniques provide a good and sometimes even better enhancement in contrast but at the cost of perceptual degradation and some noisy artifacts. It is important to note that here a constraint of *PQM* being close to 10 is being applied to obtain target output (any excursion on either side

of value 10 shall be considered visual degradation). The DSR-based technique is found to give remarkably high trade-off between all performance metrics, and thereby outsmarts most of the existing spatial domain contrast enhancement techniques.

8.4 Empirical verification of parameter optimality

Selection of the double-well parameters is an important aspect of the proposed technique. However, the authors do not claim that this is the only possible way of selecting double-well parameters for any future application of DSR for purpose of image enhancement. Since SNR is the most common quantifier of SR, parameters have been selected on the condition of maximising the SNR expression while ascertaining the condition that input is of subthreshold nature. Since parameters a and b that are optimal to maximise SNR, they are dependent on image statistics. This particular selection of parameters ensures performance of the proposed technique and has also been validated empirically. This approach for selection of parameters may be improved or tuned by further deliberation. To show that the parameters selected by the proposed approach give optimal performance, we found the performance metrics by varying parameter a and iteration count, keeping other parameters constant (tabulated in Table 4 for input image shown in Fig. 4a). It was found that the values of a smaller or larger than $a = 2\sigma_0^2$, took much larger iteration count to reach the target performance values as high as that obtained using $a = 2\sigma_0^2$. This implies that although optimal performance may be obtained by using other values of a, it would require much more iteration and consequently more computation.

8.5 Computational complexity

Computational complexity, here, is being gauged in terms of number of iterations required to reach the target optimal performance metrics. When compared with the non-DSR-based technique [18], the number of iteration in DSR-based technique was found to be less. Table 5 shows time taken to compute the outputs of existing benchmark methods using Intel Core^{TM}2 Duo CPU 3.25 GB of RAM. It can be inferred that for both images of size 445×816 and 512×512, respectively, the time cost of DSR-based

Table 5 Time cost (in seconds) using DSR in comparison with various other techniques for Figs. 3d and 5g

Methods	DSR	CLAHE	Gamma	Retinex	MSR	MHPF	EPMD	Photoshop	SSR
Fig. 3d	8.9	2.7	2.8	9.85	25.83	6.91	11.53	0.8	19.5
Fig. 5g	6.5	3.35	3.83	6.33	7.66	5.13	10.8	0.7	21.20

algorithm is greater than some of the techniques and lesser than some, but since this is at the advantage of improved perceptual quality output, this complexity can be considered acceptable.

It should be noted that experiments on many low-contrast and dark images showed that the optimum computation complexity depends greatly on the input image statistics. This is because of the selection of sampling time period Δt as per the darkness or contrast of the image. Since Δt plays the role of incremental noise scaling factor, if the image is too dark, a larger value of Δt maybe used to reach the proximity of target output in fewer iteration. For example, on the flowers images (Fig. 3*d*), using a value of $\Delta t = 0.01$, target result is obtained after five iterations, while using a value of $\Delta t = 0.005$, target output is obtained after nine iterations.

The proposed DSR-based technique performs contrast enhancement on low-contrast and dark images because due low excursion of intensity values about the mean they may be considered as subthreshold signals. However, the current form of the algorithm does not enhance a bright image (i.e. an image centred about the higher side of intensity scale) as it may lead to loss of information because of over-illumination of already bright areas. Nevertheless, the algorithm may be modified to enhance an image with both under-illuminated and over-illuminated areas by incorporating adaptive local neighbourhood processing.

The algorithm has been observed to work for all dark test images. A non-zero grayvalue has been found to be scaled up nonlinearly and increased in intensity in all cases. Hence, this technique has potential of efficient performance in various specific applications such as medical imaging, remote sensing images.

9 Conclusions

In this paper, a technique using DSR in spatial domain for the enhancement of dark- and low-contrast images was proposed and investigated. The unique feature of this technique is that it tunes the intensity values according to the bistable double-well system parameters a and b and utilises internal noise because of lack of illumination of a low-contrast image. The iterative process facilitates transition of the image from noisy (low-contrast) state to good contrast state, in analogy to the inter-well transition of a particle in a bistable system. The performance of the proposed technique has been evaluated after optimisation with respect to iteration so that the output has maximum enhancement and least iteration count. It is an automatic process that not only adjusts background illumination, but also improves the contrast and colourfulness while preserving perceptual quality. It can be inferred that the proposed DSR-based technique gives remarkable performance over the existing contrast enhancement techniques in terms of enhancement and visual information. The DSR-based technique is highly suitable for dark, coloured as well as grayscale images having varying dynamic ranges.

10 References

1 Gonzales, R.C., Woods, E.: 'Digital image processing' (Addison-Wesley, Reading, MA, 1992)
2 Lim, J.S.: 'Two-dimensional signal and image processing' (Prentice-Hall, Englewood Cliffs, NJ, 1990)
3 Jobson, D., Rahman, Z., Woodell, G.: 'Properties and performance of a center/surround retinex', *IEEE Trans. Image Process.*, 1997, **6**, (3), pp. 451–462
4 Wolf, S., Ginosar, R., Zeevi, Y.: 'Spatio-chromatic image enhancement based on a model of human visual information system', *J. Vis. Commun. Image Represent.*, 1998, **9**, (1), pp. 25–37
5 Benzi, R., Sutera, A., Vulpiani, A.: 'The mechanism of stochastic resonance', *J. Phys. A*, 1981, **14**, pp. L453–L457
6 Bulsara, A.R., Gammaitoni, L.: 'Tuning in to noise', *Phys. Today*, 1996, **49**, pp. 39–45
7 Gammaitoni, L., Hanggi, P., Jung, P., Marchesoni, F.: 'Stochastic resonance', *Rev. Mod. Phys.*, 1998, **70**, pp. 223–270
8 Hongler, M., Meneses, Y., Beyeler, A., Jacot, J.: 'Resonant retina: exploiting vibration noise to optimally detect edges in an image', *IEEE Trans. Pattern Anal. Mach. Intell.*, 2003, **25**, (9), pp. 1051–1062
9 Ye, Q., Huang, H., He, X., Zhang, C.: 'A SR-based radon transform to extract weak lines from noise images'. Proc. IEEE Int. Conf. on Image Processing, Barcelona, Spain, 2003, vol. 5, no. 6, pp. 1849–1852
10 Ye, Q., Huang, H., Zhang, C.: 'Image enhancement using stochastic resonance'. Proc. IEEE Int. Conf. Image Processing, Singapore, 2004, vol. 1, pp. 263–266
11 Peng, R., Chen, H., Varshney, P.K.: 'Stochastic resonance: an approach for enhanced medical image processing'. IEEE/NIH Life Science Systems and Applications Workshop, 2007, vol. 1, pp. 253–256
12 Rallabandi, V.P.S.: 'Enhancement of ultrasound images using stochastic resonance based wavelet transform', *Comput. Med. Imaging Graph.*, 2008, **32**, pp. 316–320
13 Rallabandi, V.P.S., Roy, P.K.: 'Magnetic resonance image enhancement using stochastic resonance in Fourier domain', *Comput. Med. Imaging Graph.*, 2010, **28**, pp. 1361–1373
14 Ryu, C., Konga, S.G., Kimb, H.: 'Enhancement of feature extraction for low-quality fingerprint images using stochastic resonance', *Pattern Recognit. Lett.*, 2011, **32**, (2), pp. 107–113
15 Simonotto, E., Riani, M., Charles, S., Roberts, M., Twitty, J., Moss, F.: 'Visual perception of stochastic resonance', *Phys. Rev. Lett.*, 1997, **78**, (6), pp. 1186–1189
16 Piana, M., Canfora, M., Riani, M.: 'Role of noise in image processing by the human perceptive system', *Phys. Rev. E*, 2000, **62**, (1), pp. 1104–1109
17 McNamara, B., Wiesenfeld, K.: 'Theory of stochastic resonance', *Phys. Rev. A*, 1989, **39**, (9), pp. 4854–4869
18 Jha, R.K., Biswas, P.K., Chatterji, B.N.: 'Contrast enhancement of dark images using stochastic resonance', *IET Image Process., IEE*, 2012, **6**, (3), pp. 230–237
19 Benzi, R., Parisi, G., Sutera, A., Vulpiani, A.: 'Stochastic resonance in climate change', *Tellus*, 1982, **34**, pp. 10–16
20 Rouvas-Nicolis, C., Nicolis, G.: 'Stochastic resonance', *Scholarpedia*, 2007, **2**, (11), pp. 1474
21 Risken, H.: 'The Fokkar Plank equation' (Springer Verlag, Berlin, 1984)
22 McDonnell, M.D., Stocks, N.G., Pearce, C.E.M., Abbott, D.: 'Stochastic resonance: from suprathreshold stochastic resonance to stochastic signal quantization' (Cambridge University Press, New York, 1990)
23 Jung, P., Hanggi, P.: 'Amplification of small signal via stochastic resonance', *Phys. Rev. A*, 1991, **44**, (12), pp. 8032–8042
24 Gard, T.C.: 'Introduction to stochastic differential equations' (Marcel-Dekker, New York, 1998)
25 Wang, Z., Sheikh, H.R., Bovik, A.C.: 'No-reference perceptual quality assessment of jpeg compressed images'. Proc. IEEE Int. Conf. on Image Processing, New York, USA, 2002, vol. 1, pp. 477–480
26 http://www.facweb.iitkgp.emet.in/~jay/CES/README.html (accessed 7th July 2011)
27 Mukherjee, J., Mitra, S.K.: 'Enhancement of color images by scaling the dct coefficients', *IEEE Trans. Image Process.*, 2008, **17**, (10), pp. 1783–1794
28 Susstrunk, S., Winkler, S.: 'Color image quality on the internet'. Proc. IS&T/SPIE Electronic Imaging: Internet Imaging V, 2004, vol. 5304, pp. 118–131
29 Farbman, Z., Fattal, R., Lischinski, D., Szeliski, R.: 'Edge-preserving decompositions for multi-scale tone and detail manipulation', *ACM Trans. Graph.*, 2008, **27**, (3), pp. 1–10
30 Zuiderveld, K.: 'Contrast limited adaptive histogram equalization' (Academic Press Professional Inc., San Diego, CA, USA, 1994), pp. 474–485, http://portal.acm.org/citation.cfm?id = 180895.180940
31 Jobson, D.J., Rahman, Z., Woodell, G.A.: 'A multi-scale retinex for bridging the gap between color images and the human observation of scenes', *IEEE Trans. Image Process.*, 1997, **6**, (7), pp. 965–976
32 Yang, C.: 'Image enhancement by the modified high-pass filtering approach', *Optik – Int. J. Light Electron. Opt.*, 2009, **120**, (17), pp. 886–889
33 http://www.cs.huji.ac.il/_danix/epd/ (accessed 15th August 2011)